# ZnO:Sb/ZnO:Ga Light Emitting Diode on *c*-Plane Sapphire by Molecular Beam Epitaxy

Zheng Yang, Sheng Chu, Winnie V. Chen[1], Lin Li, Jieying Kong, Jingjian Ren, Paul K. L. Yu[1], and Jianlin Liu*

*Quantum Structures Laboratory, Department of Electrical Engineering, University of California, Riverside, CA 92521, U.S.A.*
[1]*Department of Electrical and Computer Engineering, University of California, San Diego, La Jolla, CA 92093, U.S.A.*

Received December 20, 2009; accepted February 15, 2010; published online March 5, 2010

p-type Sb-doped ZnO (ZnO:Sb)/n-type Ga-doped ZnO (ZnO:Ga) junctions were grown on *c*-plane sapphire substrates using plasma-assisted molecular-beam epitaxy. Mesa geometry light emitting diodes (LEDs) were fabricated using standard photolithography and lift-off process, with ohmic contacts achieved using Au/Ni and Au/Ti for top ZnO:Sb and bottom ZnO:Ga layers, respectively. Rectifying current–voltage characteristics were achieved. Ultraviolet emission dominates in the electroluminescence spectra of the ZnO LED. An output power of ~32 nW at an applied current of 60 mA was demonstrated. The enhanced output power, as compared to those made on silicon substrates, is attributed to the improved ZnO film quality on sapphire substrates, which is confirmed by X-ray diffraction rocking curve studies.
© 2010 The Japan Society of Applied Physics

DOI: 10.1143/APEX.3.032101

ZnO is a promising candidate material for ultraviolet optoelectronic devices, due to its large exciton binding energy and suitable bandgap.[1,2] Reliable p-type doping in ZnO is indispensible for ZnO optoelectronic device technologies. Sb was theoretically proposed to be a reliable acceptor dopant in ZnO based on density-function calculations,[3] which was experimentally confirmed subsequently.[4–7] Functional prototype devices based on p-type ZnO:Sb materials have been demonstrated in recent years, such as photodetectors,[8,9] light-emitting diodes (LEDs),[10–13] and random lasing devices,[14] indicating Sb is an effective dopant for p-type doping in ZnO. Currently, the low output power is one of the limiting factors for ZnO LEDs using Sb as p-dopant. The best output power previously obtained in ultraviolet-emission-dominated LED with ZnO:Sb p-layer was only ~1 nW at 100 mA injection current,[12] which is possibly due to the low film quality for the ZnO layers grown on Si(100) substrates. Due to much reduced lattice mismatch between ZnO and *c*-plane sapphire compared with that between ZnO and Si(100) and the starting hexagonal sapphire lattice in favor of ZnO Wurtzite structure growth, ZnO diodes on sapphire shall have significantly better film quality, leading to enhanced light output. In this study ZnO:Sb/ZnO:Ga LEDs on *c*-plane sapphire substrates with significantly improved output power of ~32 nW at 60 mA are reported.

p-ZnO:Sb/n-ZnO:Ga homojunctions were grown on *c*-plane sapphire substrates using plasma-assisted molecular-beam epitaxy (MBE). Sapphire substrates were firstly chemically cleaned in an aqua regia ($HNO_3 : HCl = 1 : 3$) solution at 150 °C for 20 min, then rinsed in de-ionized water, and finally dried with a nitrogen gun and transferred into the MBE load-lock chamber. The growth began with a 5 min deposition of seeding ZnO at 350 °C, followed by a regular buffer layer growth at 620 °C. The subsequent n-ZnO:Ga and p-ZnO:Sb layers were grown at 620 and 550 °C, respectively. The effusion cell temperatures of Zn, Ga, and Sb are 380, 560, and 420 °C, respectively. The Zn beam flux is on the order of $10^{-7}$ Torr, while Ga and Sb beam fluxes are on the order of $10^{-9}$ Torr. The ZnO:Ga and ZnO buffer layers were grown under near stoichiometric condition while the ZnO:Sb layer was grown under oxygen rich condition. The thickness of the buffer, ZnO:Ga, and ZnO:Sb is 400, 300, and 200 nm, respectively. Post growth thermal annealing was performed at 750 °C in oxygen ambient. Mesa geometry LEDs with a mesa size of $800 \times 800\,\mu m^2$ were fabricated using standard photolithography and lift-off processes. Au/Ti and Au/Ni[15] were deposited using e-beam evaporation on n-ZnO:Ga layer and p-ZnO:Sb layer, respectively, as electrical contacts. Ohmic contacts were achieved after rapid thermal annealing process. Figure 1(a) shows the schematic of the device structure. Secondary ion mass spectroscopy (SIMS) measurements were performed on a dedicated LED device with a Cameca IMS 4.5F system. Figure 1(b) shows the SIMS distribution profile of elements O, Zn, Sb, and Ga along the depth direction. The elemental distribution is consistent with the designed device structure. The slight Sb diffusion is due to the high temperature annealing after growth.[15]

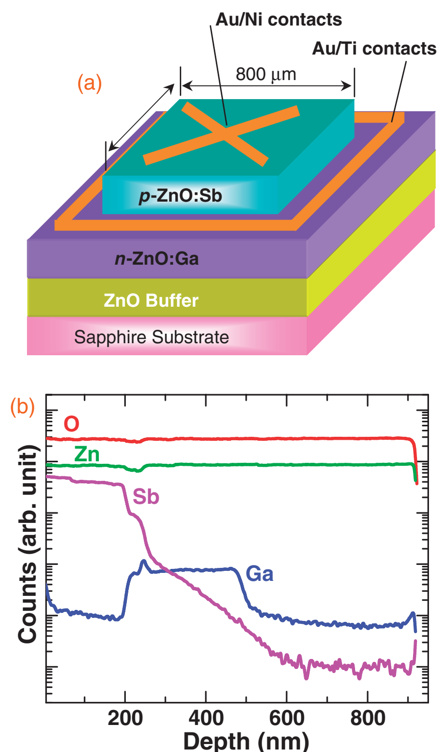


**Fig. 1.** (a) Schematic of the ZnO LED structure. (b) SIMS spectra of the ZnO LED with distribution of elemental O, Zn, Sb, and Ga vs depth.

*E-mail address: jianlin@ee.ucr.edu


© 2010 The Japan Society of Applied Physics

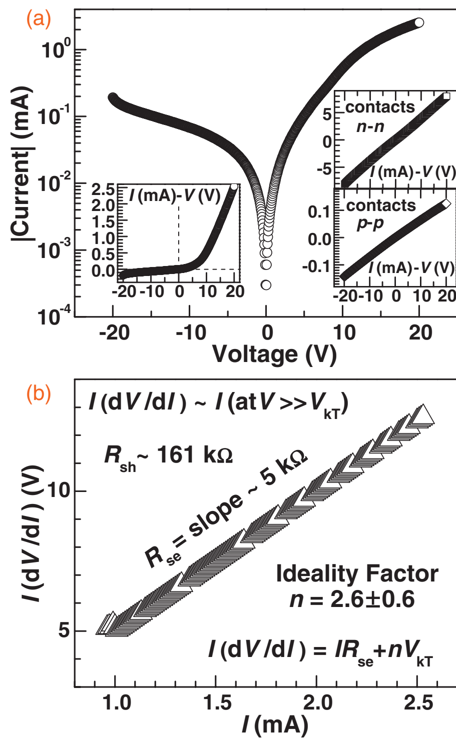


**Fig. 2.** (a) $I$–$V$ characteristic of the ZnO LED in semi-logarithmic plot. Left inset: $I$–$V$ characteristic of the ZnO LED in linear plot. Top right inset: $I$–$V$ characteristic between contacts on ZnO:Ga layer (labeled as n–n contacts). Bottom right inset: $I$–$V$ characteristic between contacts on ZnO:Sb layer (labeled as p–p contacts). The linear $I$–$V$ behaviors in right insets indicate the formation of ohmic contacts. (b) Plot of $I(dV/dI)$ versus $I$. The ideality factor $n$ and series resistance $R_{se}$ are derived from the intercept and slope fitting.

Current–voltage ($I$–$V$) characteristics of the devices were measured by an Agilent 4155C semiconductor parameter analyzer. Figure 2(a) shows the $I$–$V$ characteristics of an LED device in semi-logarithmic drawing. The left inset in Fig. 2(a) shows the same curve but in linear plot. Rectifying behavior is observed. The top right and bottom right insets in Fig. 2(a) show the linear $I$–$V$ curves of n–n contacts on ZnO:Ga layer and p–p contacts on ZnO:Sb layer, respectively, indicating the formation of Ohmic contacts. The Ohmic behavior of metal contacts on top of ZnO excludes the possibility of formation any Schottky junctions in the device. In practice the $I$–$V$ characteristics of homojunction diodes follow the equation,

$$I = I_S \exp\left(\frac{V - IR_{se}}{nV_T}\right) + \frac{V - IR_{se}}{R_{sh}}, \qquad (1)$$

where $I_S$ is the saturation current, $n$ is the ideality factor, $V_T = k_B T/e$ is the thermal voltage (with $k_B$ Boltzmann constant, $T$ temperature, and $e$ electron charge), $R_{se}$ is the series resistance, and $R_{sh}$ is the shunt resistance.[16] The differential resistance can be derived as

$$\frac{dV}{dI} = R_{se} + \left\{\frac{1}{R_{sh}} + \frac{1}{nV_T}\left[\left(1 + \frac{R_{se}}{R_{sh}}\right)I - \frac{1}{R_{sh}}V\right]\right\}^{-1}.$$

In case of very large shunt resistance $R_{sh}$, it can be approximated as,

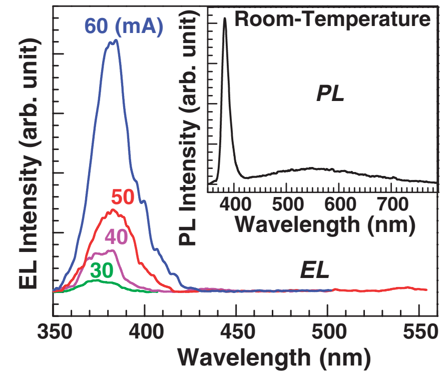


**Fig. 3.** Room-temperature EL of the ZnO LED. Inset: Room-temperature PL of the ZnO LED.

$$\frac{dV}{dI} \approx R_{se} + \frac{nV_T}{I}. \qquad (2)$$

Figure 2(b) shows the plot of $I(dV/dI)$ versus $I$. The slope and intercept on vertical-axis of this plot are used to obtain the series resistance $R_{se}$ and the ideality factor $n$. $R_{se} \approx 5\,\text{k}\Omega$ is achieved from the fitted slope of the data plot. The ideality factor $n = 2.6 \pm 0.6$ is estimated from the fitted intercept divided by the thermal voltage. The deviation comes from the extrapolation fitting uncertainty. Finally, the shunt resistance $R_{sh}$ is approximately calculated as $R_{sh} = dV/dI|_{I\to 0, V\to 0} - R_{se} \approx 161\,k\Omega$. The series resistance value is large, which is possibly due to the relatively high resistance of the ZnO:Sb p-layer. The turn on voltage of the LED from the rectification $I$–$V$ curve is ~6 V. The large turn on voltage is also partially due to the large series resistance.

The electroluminescence (EL) and photoluminescence (PL) measurements were carried out using a PL/EL system composed of an Oriel monochromator, a photomultiplier detector, a lock-in amplifier, and a chopper. An external HP E3630A dc power supply was used to input current for EL measurements. A 325-nm wavelength (Kimmon) He–Cd laser was used as an excitation source for PL measurements. Figure 3 shows the EL spectra of an LED device, with injected current ranging from 30 to 60 mA. The near-band-edge ultraviolet emissions dominate in the EL spectra and the intensity increases with the increase of the injection current. The EL peak position slightly red-shifts from 3.32 eV (374 nm) at small injection current (30 mA) to 3.23 eV (384 nm) at large injection current (60 mA), which is attributed to heat induced bandgap shrinkage.[11,12] The inset of Fig. 3 shows the PL spectrum of the sample. Besides the near-band-edge emission, a deep level emission at ~550 nm was observed in the PL spectrum but not in the EL spectra. The PL spectrum is mainly from the top ZnO:Sb layer, because the penetration depth of the 325 nm laser in ZnO is ~100 nm,[17] which is about half that of the ZnO:Sb layer thickness. This indicates that the band-to-band recombination is dominant at forward bias in the diode operation.

The output power of the EL was measured and calibrated with an Ocean Optics integral sphere. The device shows a ~32 nW output at 60 mA injection current. This value is much larger than the previously reported ZnO:Sb/ZnO:Ga junction LED on Si (~1 nW output at 100 mA).[12]


© 2010 The Japan Society of Applied Physics

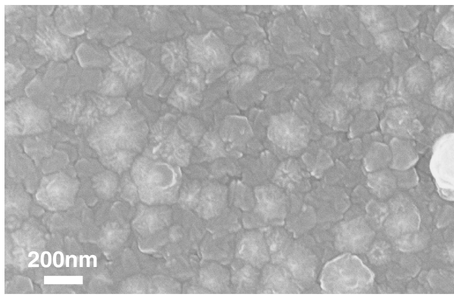


**Fig. 4.** Top-view SEM image of the ZnO LED.

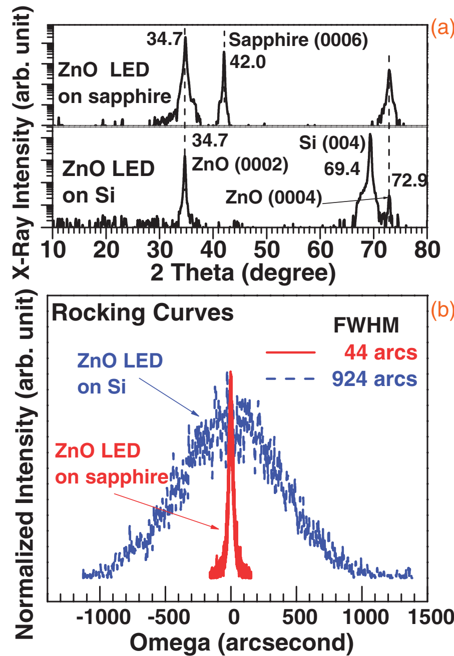


**Fig. 5.** XRD patterns of the device sample discussed in the paper and a reference LED sample on Si previously discussed in ref. 12 in (a) $2\theta$ scans and (b) rocking curve scans of ZnO(0002) peak.

The orders of magnitude improvement in light emission is due to the improved film quality. To clarify this, scanning electron microscope (SEM) and X-ray diffraction (XRD) measurements were carried out. The top view of the SEM image of the device is shown in Fig. 4. The morphology of the thin film is similar to those grown on Si,[10–12,14] which consists of closely-packed nano-columns. However, these well-aligned nano-columns exhibit high quality from XRD measurements performed using a Philips X-ray diffractometer in both $2\theta$ and $\omega$ (rocking curve) scan geometries. Figure 5(a) shows the XRD patterns of the device sample and a reference ZnO LED sample on Si (discussed in ref. 12). The two samples show similar XRD $\theta$–$2\theta$ scan patterns (except for the substrate peak difference) with the *c*-orientation dominating. However, the two samples show significantly different full-width-at-half-maximum (FWHM) peaks in XRD rocking curve scans of ZnO(0002) peaks, as shown in Fig. 5(b). The device sample discussed in this paper shows a much smaller FWHM (~44 arcsec) than the sample[12] on Si (~924 arcsec). This is due to the employment of *c*-plane sapphire substrates instead of Si substrates. The improved crystallinity reduces non-radiative recombination probability, leading to the enhanced output power. This research verifies that ZnO crystallinity is another dominating factor for future high efficiency ZnO optoelectronic devices, besides the efficiency issue of p-type doping in ZnO.

In summary, ZnO LEDs were fabricated based on p-ZnO:Sb/n-ZnO:Ga junctions grown on *c*-plane sapphire substrates using plasma-assisted MBE. $I$–$V$ characteristics show typical diode rectifying behavior. The ideality factor, series resistance, and shunt resistance of the ZnO LED are estimated to be $n = 2.6 \pm 0.6$, $R_{se} \approx 5\,k\Omega$, and $R_{sh} \approx 161\,k\Omega$, respectively. Ultraviolet emission dominates in the EL spectra of the ZnO LED. The ZnO LED shows an output power of ~32 nW at 60 mA injection current (compared to ~1 nW at 100 mA for ZnO grown on Si), as a result of high crystallinity of ZnO nano-columns grown on sapphire. Further improvement of light output may be achieved by developing single-crystalline ZnO p–n junctions on sapphire.

**Acknowledgments** This work was supported by Department of Energy (DOE) under grant No. DE-FG02-08ER46520, by Army Research Office Young Investigator Program (ARO-YIP) under grant No. W911NF-08-1-0432, by National Science Foundation (NSF) under grant No. ECCS-0900978, and by Office of Naval Research/Defense Microelectronics Activity (ONR/DMEA) through the Center of Nanomaterials and Nanodevice (CNN) under the award No. H94003-08-2-0803 in U.S.A.

1) D. C. Look: Mater. Sci. Eng. B **80** (2001) 383.
2) C. Klingshirn: Phys. Status Solidi B **244** (2007) 3027.
3) S. Limpijumnong, S. B. Zhang, S. H. Wei, and C. H. Park: Phys. Rev. Lett. **92** (2004) 155504.
4) F. X. Xiu, Z. Yang, L. J. Mandalapu, D. T. Zhao, J. L. Liu, and W. P. Beyermann: Appl. Phys. Lett. **87** (2005) 152101.
5) F. X. Xiu, Z. Yang, L. J. Mandalapu, D. T. Zhao, and J. L. Liu: Appl. Phys. Lett. **87** (2005) 252102.
6) P. Wang, N. Chen, Z. Yin, R. Dai, and Y. Bai: Appl. Phys. Lett. **89** (2006) 202102.
7) W. Guo, A. Allenic, Y. B. Chen, X. Q. Pan, Y. Che, Z. D. Hu, and B. Liu: Appl. Phys. Lett. **90** (2007) 242108.
8) L. J. Mandalapu, F. X. Xiu, Z. Yang, D. T. Zhao, and J. L. Liu: Appl. Phys. Lett. **88** (2006) 112108.
9) L. J. Mandalapu, Z. Yang, F. X. Xiu, D. T. Zhao, and J. L. Liu: Appl. Phys. Lett. **88** (2006) 092103.
10) L. J. Mandalapu, Z. Yang, S. Chu, and J. L. Liu: Appl. Phys. Lett. **92** (2008) 122101.
11) S. Chu, J. H. Lim, L. J. Mandalapu, Z. Yang, L. Li, and J. L. Liu: Appl. Phys. Lett. **92** (2008) 152103.
12) J. Kong, S. Chu, M. Olmedo, L. Li, Z. Yang, and J. L. Liu: Appl. Phys. Lett. **93** (2008) 132113.
13) J. Z. Zhao, H. W. Liang, J. C. Sun, J. M. Bian, Q. J. Feng, L. Z. Hu, H. Q. Zhang, X. P. Liang, Y. M. Luo, and G. T. Du: J. Phys. D **41** (2008) 195110.
14) S. Chu, M. Olmedo, Z. Yang, J. Kong, and J. L. Liu: Appl. Phys. Lett. **93** (2008) 181106.
15) L. J. Mandalapu, Z. Yang, and J. L. Liu: Appl. Phys. Lett. **90** (2007) 252103.
16) E. F. Schubert: *Light-Emitting Diodes* (Cambridge University Press, Cambridge, U.K., 2006) 2nd ed., p. 63.
17) C. J. Pana, C. W. Tu, J. J. Song, G. Cantwell, C. C. Lee, B. J. Pong, and G. C. Chi: J. Cryst. Growth **282** (2005) 112.

 © 2010 The Japan Society of Applied Physics